

Measurement Note

NPL Report MN 06

Development of Test Methods for Measuring Thick Section Tensile and Compression Properties of Polymer Matrix Composites

The use of polymer matrix composites (PMCs) has primarily involved thin membrane structures, but recent developments have seen an expansion in the use of composite materials in structural applications involving thick sections in excess of 20 mm, often complex in shape. The general perception has been to consider through-thickness properties with thick composites as problematical and difficult to measure, whereas in fact an equally important issue relates to the measurement of in-plane properties and the effect of physical size of test specimens on measured data. Although extensive developmental work has been undertaken worldwide into test methods and design procedures for in-plane properties of thin laminates, there are no standard test methods available that provide guidance on testing of thick composite sections. The approach generally adopted has been to use existing standards, developed for testing small laboratory-scale specimens, with non-standard (i.e. larger) specimen geometries. A major concern relates to whether data generated from standards for relatively thin specimens are equivalent to or representative of thick section mechanical behaviour.

This Measurement Note details work undertaken to develop tension and compression test methods suitable for testing ~20 mm thick carbon fibre-reinforced plastic (CFRP) laminates in support of the design of composite components comprising of thick material sections. The work has been carried out to evaluate the scaling effect of increasing coupon size (in-plane dimensions and thickness) for distributed ply laminates and effect of ply-level scaling i.e. the blocking together of plies of the same orientation.

M R L Gower and R M Shaw

**February 2011
Issue 2**

© Queen's Printer and Controller of HMSO, 2011.
Issue 2

ISSN No. 1754-3002

National Physical Laboratory
Hampton Road, Teddington, Middlesex, TW11 0LW

INTRODUCTION

The use of polymer matrix composites (PMCs) has primarily involved thin membrane structures, but recent developments have seen an increase in the use of composite materials in structural applications involving sections in excess of 20 mm thick and often complex in shape. A major concern relates to whether data generated from standards for relatively thin specimens are equivalent to or representative of thick section mechanical behaviour. Measurement of in-plane properties of thick sections can pose considerable problems from a testing perspective unless scaling effects are understood. Thick laminated sections also pose particular problems in relation to mechanical testing, as the large size of the test pieces often requires high load capacity testing facilities, which are not readily accessible for most organisations, large test fixtures and increased difficulties associated with load introduction into the specimen. The lack of suitable test methods has resulted in a shortage of reliable engineering data for large structural applications.

This Measurement Note details work undertaken to develop tension and compression test methods suitable for testing ~20 mm thick carbon fibre-reinforced plastic (CFRP) laminates in support of the design of composite components comprising of thick material sections. The work has been designed to evaluate the scaling effect of increasing coupon size (thickness) for distributed ply laminates and effect of ply-level scaling i.e. the blocking together of plies of the same orientation.

MATERIAL AND LAY-UP DETAILS

The material system used in this study was SE84 LV unidirectional carbon fibre-reinforced epoxy pre-preg supplied by Gurit Holdings AG as an industrial co-funding contribution to the project. Baseline tensile and compressive data for 'thin' quasi-isotropic (QI) SE84 LV laminates, manufactured in an autoclave according to the material supplier's recommended cure cycle, were generated for subsequent comparison with the 'thick' material data. Tensile data were measured according to ISO 527-4 [1] using a QI lay-up of $[+45^\circ/0^\circ/-45^\circ/90^\circ]_s$ (~2.5 mm thick) and compressive data were measured according to ISO 14126 [2] using a QI lay-up of $[+45^\circ/0^\circ/-45^\circ/90^\circ]_{2s}$ (~5 mm thick). The 'thin' laminate data are shown in Table 1.

In order to investigate the effect of lay-up on laminate stiffness and strength, three variations of a QI lay-up have been considered;

- (i) $[+45^\circ/0^\circ/-45^\circ/90^\circ]_{8s}$ - distributed QI (sub-laminate scaling),
- (ii) $[+45^\circ_n/0^\circ_n/-45^\circ_n/90^\circ_n]_{ms}$ - blocked QI (ply-level scaling) where $n = 8$ and $m = 1$ (tension), and $n = 4$ and $m = 2$ (compression).

Distributed and blocked QI lay-ups were tested for both tension and compression modes and the respective lay-ups are shown in Table 2. The degree of blocking was reduced from $n = 8$ for tension to $n = 4$ for compression to avoid ply splitting observed for the $n = 8$ tensile coupons (see Panel & Specimen Preparation). As extremely large loads (~5

Table 1: Tensile and Compressive Property Data for Thin QI SE84 LV Laminates

Mode	Lay-up	Modulus (GPa)	Strength (MPa)	Poisson's ratio
Tension	$[+45^\circ/0^\circ/-45^\circ/90^\circ]_s$	44.2 (1.3%)	551 (4.0%)	0.35 (16%)
Compression	$[+45^\circ/0^\circ/-45^\circ/90^\circ]_{2s}$	44.0 (5.4%)	454 (2.7%)	—

N.B. Tensile tests undertaken according to ISO 527-4 [1], compressive tests undertaken according to ISO 14126 [2]

Table 2: Thick Section Lay-up Details

Loading Mode	Scaling Type	Lay-up	Nominal Thickness (mm)	Fibre Volume Fraction, V_f (%)
Tension	Sub-laminate	$[+45^\circ/0^\circ/-45^\circ/90^\circ]_{8s}$	19.75	55.1
	Ply level	$[+45^\circ_8/0^\circ_8/-45^\circ_8/90^\circ_8]_s$		55.0
Compression	Sub-laminate	$[+45^\circ/0^\circ/-45^\circ/90^\circ]_{8s}$	19.44	53.0
	Ply level	$[+45^\circ_4/0^\circ_4/-45^\circ_4/90^\circ_4]_{2s}$		53.3

MN and ~2 MN in tension and compression, respectively) are required to fail thick unidirectional (UD) specimens, it was therefore decided that testing would be limited to QI lay-ups only. Waisting the width of UD specimens was considered as a means of reducing the failure loads, but this tends to result in longitudinal splitting of specimens prior to failure.

THICK SPECIMEN DESIGN

The following sections detail the design of tension and compression specimens suitable for testing ~20 mm thick laminates.

Tension

From the outset of the design process, the size and shape of tensile coupons were limited by the availability of test machines with sufficiently high load capacity to achieve failure and also grips with an equally high load rating. In addition, the size of the test specimens was limited by the maximum size of panel (600 x 300 mm) that could be manufactured in the NPL autoclave facility and also the requirement to be able to test a reasonable number of specimens.

On the assumption that a 20 mm thick distributed QI laminate would fail at a similar magnitude of stress as a thin laminate of the same unit lay-up, the approximate tensile failure stress for a thick laminate was set at a level equivalent to that obtained from measured data for ~2.5 mm thick material. From this failure stress the failure load for specimens with a given cross-sectional area could be calculated. Consideration was then given to the width of the gauge-section to

Determination of end-tab length [3]:

$$L_T = \frac{\sigma_T w_g t_g}{2 w_T \sigma_s} \quad (1)$$

where:

L_T = length of end-tab

σ_T = tensile strength of 'thin' laminate (measured 551 MPa)

w_g = width of gauge section

t_g = thickness of gauge-section (~20 mm)

w_T = width of end-tab region

σ_s = shear strength of adhesive or end-tab material (adhesive = 32 MPa)

ensure that the specimen was wide enough to provide a region of reasonably uniform strain, but as narrow as possible to limit the load required to achieve failure. A gauge width of 50 mm was chosen and the length of the parallel sided gauge-section was set to 50 mm. In addition, to ensure failure in the gauge-section, the width of the end-tab region was set to 90 mm. This also allowed 3 specimens to be cut from one panel. The minimum length of the end-tabs was then calculated [3] using Equation (1) which equates the shear strength of the adhesive used to bond the end-tabs to the tensile strength of the laminate. The laminate tensile strength, σ_T , was 551 MPa from thin laminate data and the adhesive shear strength, σ_s , was 32 MPa. The minimum length of the end-tabs was calculated to be 96 mm. A safety factor of ~1.5 was applied to this length and thus the end-tab length was set to 150 mm. The length of specimens was set to 600 mm (maximum panel length). The transition from end-tab regions to gauge-

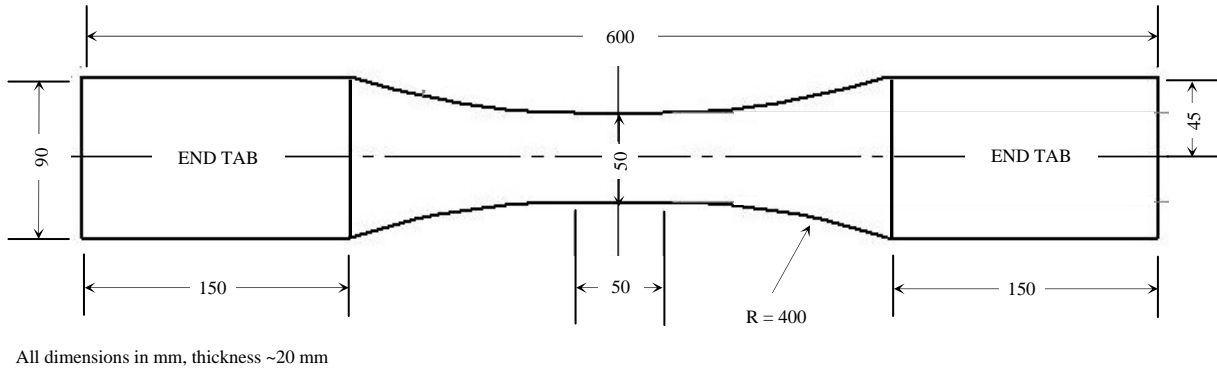


Figure 1: Geometry and dimensions of thick tensile specimen



Figure 2: Comparison between standard multidirectional tensile specimen (~5 mm thick) and thick tensile specimen (~20 mm)

section was made as smooth as possible to avoid stress concentrations and thus the largest radius possible, $R = 400$ mm, was chosen. The final thick coupon design is shown schematically in Figure 1. A comparison between the thick tensile coupon design (prior to being end-tabbed) to a standard 'thin' coupon as per ISO 527-4 [1] is shown in Figure 2.

Compression

Compression data for ~ 5 mm thick distributed QI material were generated using a four pillar die set end-loading jig. As for the tension specimen design it was assumed that the compressive failure stress for a 20 mm thick distributed QI laminate would be of a similar magnitude of stress as for a thin laminate of the same unit lay-up. Therefore, for design purposes the approximate compressive failure

stress for a thick laminate was set at a level equivalent to that obtained from measured data for ~5 mm thick material. As for the design of the tensile coupon consideration was given to maximising the number of specimens that could be extracted from a 600 x 300 mm panel. The length of specimens was derived from calculating the maximum length of the gauge-section below which Euler buckling would not occur whilst ensuring a sufficient length of gauge section to achieve a region of strain uniformity in which to position strain gauges and make strain measurements. Equation (2) was used to calculate the maximum gauge length using values of σ_c , E_c and G_{13} measured from 'thin' section distributed QI lay-up laminate tests. The gauge-section length for both lay-ups was calculated for the distributed QI case as this was the lay-up with the highest anticipated compressive strength giving the shortest gauge length i.e. for the $n = 4$ blocked QI lay-up the

Determination of maximum gauge length [2]:

$$L_{\max} \leq 0.9069 t \sqrt{\left(1 - \frac{1.2 \sigma_c}{G_{13}}\right) \left(\frac{E_c}{\sigma_c}\right)} \quad (2)$$

where:

- L_{\max} = maximum length of gauge section
- σ_c = compressive strength of 'thin' laminate (measured 454 MPa)
- E_c = compressive modulus of laminate (measured 44 GPa)
- G_{13} = through-thickness shear modulus (3.01 GPa)
- t = thickness of laminate (19.65 mm)

compressive failure strength was anticipated to be lower thus giving a higher maximum gauge-length. As it was required to keep the specimen geometry for both distributed and

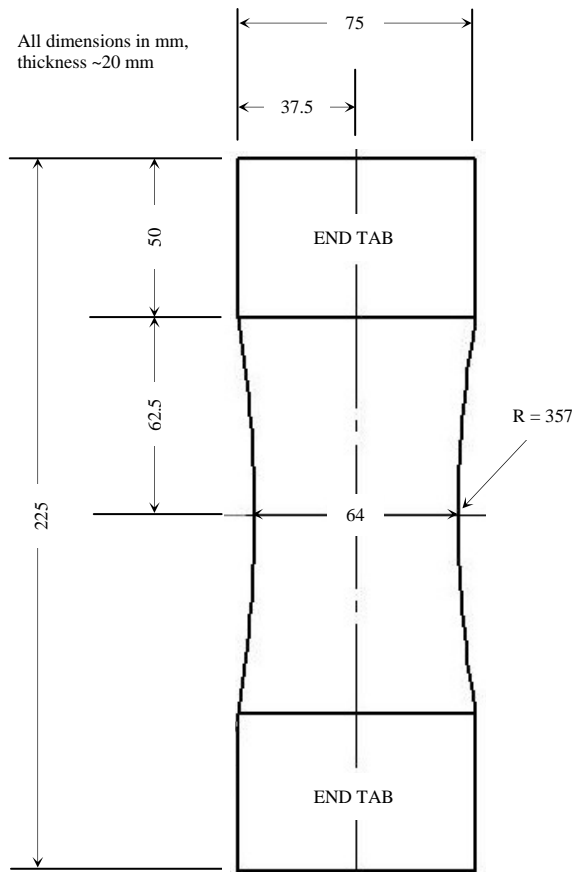


Figure 3: Geometry and dimensions of thick compression specimen

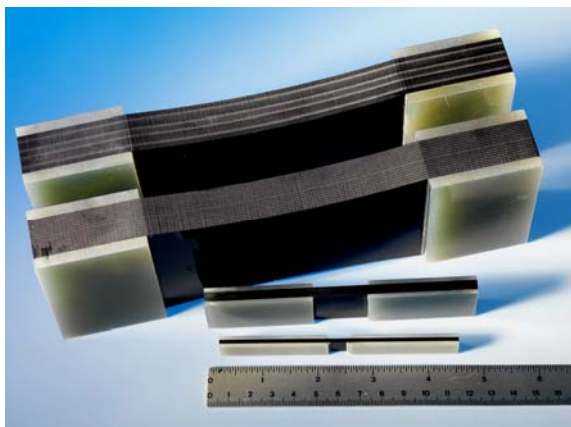


Figure 4: Comparison between standard multidirectional compression specimen (~4 mm thick) and thick compression specimen (~20 mm)

blocked lay-ups the same, the gauge-length calculated for the distributed QI laminate was chosen. This length was set at 125 mm. The length of the region of specimens supported within the end-loading blocks was set to 50 mm, which is the same as for the ~5 mm thick specimens. Therefore, the overall length of specimens was calculated to be 225 mm. As the gauge-length was fairly short (in comparison to the tensile coupons) it was not practical to have a parallel sided length in the gauge-section. The width of the gauge-section was set to 64 mm to ensure that failure occurred in the gauge-section, but that the potential of longitudinal splitting of the material was minimised. The transition from end-tab regions to the gauge-section was made as smooth as possible to avoid stress concentrations, and thus the largest radius possible, $R = 357$ mm, was chosen. The final thick coupon design is shown schematically in Figure 3. A comparison between the thick compression coupon design and standard ‘thin’ unidirectional and multidirectional coupons as per ISO 14126 [2] is shown in Figure 4.

FEA analysis

A series of finite element analyses (FEA) were undertaken for both tensile and compression coupon designs using LUSAS Composite software. The analyses were 3D, non-linear and incorporated damage analysis using the Hashin damage criterion. Models were created for distributed and blocked laminates with end-tabs and adhesive being modelled. Elastic and strength ply data for the SE84 LV material system (previously measured at NPL) were used as input into the FE models (see Table 3).

For the tensile models, a 20 MPa clamping stress was initially applied to the end-tab regions to replicate the clamping pressure applied in the experimental tests via the hydraulic grips. A total tensile load of 800 kN (Figure 5(a)) was then applied through shear via the end-tabs incrementally until the model no longer achieved convergence due to accumulated damage.

For the compressive models, a 20 MPa clamping stress was initially applied to the end-tab regions to simulate the clamping from the support blocks of the end-loaded

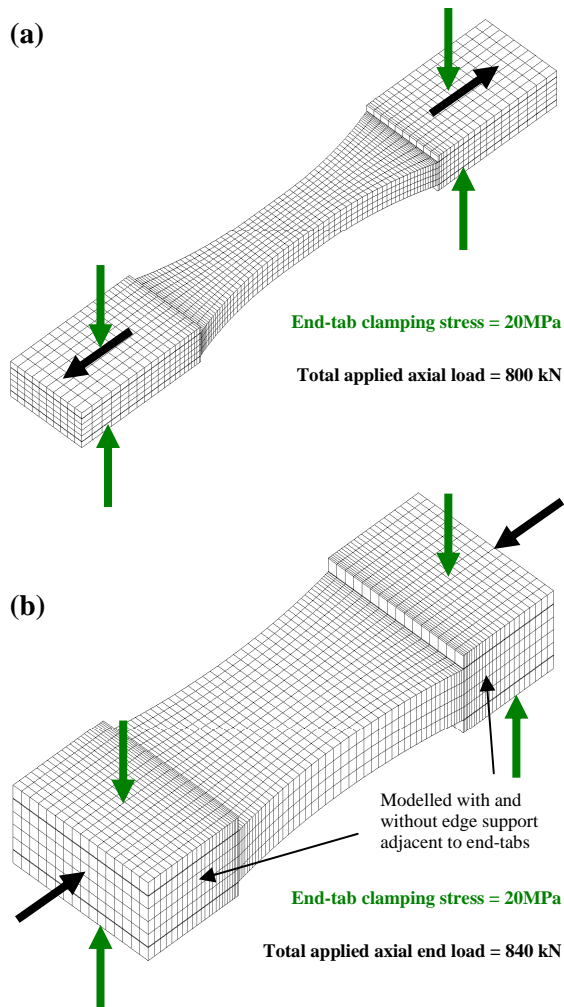


Figure 5: FEA mesh and loading for; (a) tension and (b) compression

compression jig. A total compressive load of 840 kN was then applied to the ends of the specimen (Figure 5(b)) incrementally until the model no longer achieved convergence due to accumulated damage. Compression specimens were modelled with edge restraint of the end-tab regions in order to mimic the support conditions seen in the actual tests. The FEA analyses were used to predict stress and strain distributions for comparison with data measured in experimental tests on the same coupon designs.

The LUSAS Composite FE software includes the Tsai-Wu, Tsai-Hill, Hofman, Hashin fibre and Hashin matrix failure criteria and these were used to predict progressive failure within the tensile specimen designs and for comparison to experimental results. The Tsai-Hill criterion tended to show the best agreement with experimental results in terms of failure location, but tended to over predict

Table 3: Elastic Property Data for SE84 LV Material Used in FEA Analyses

Elastic Property	Value
E_{xx}^T (GPa)	124.3 ± 4.4
E_{yy}^T (GPa)	8.14 ± 0.1
E_{zz}^T (GPa)	7.8 ± 0.12
E_{xx}^C (GPa)	110.0 ± 5.6
E_{yy}^C (GPa)	8.5 ± 0.4
E_{zz}^C (GPa)	8.3 ± 0.14
G_{xy} (GPa)	4.49 ± 0.07
G_{xz} (GPa)	3.93 ± 0.21
G_{yz} (GPa)	2.44 ± 0.10
ν_{xy}^T	0.32 ± 0.02
ν_{zx}^T	0.017 ± 0.004
ν_{zy}^T	0.505 ± 0.005
ν_{zx}^C	0.020 ± 0.009
ν_{zy}^C	0.518 ± 0.007
Strength Property (MPa)	Value
S_{xx}^T	2751 ± 32
S_{yy}^T	25 ± 9
S_{zz}^T	42 ± 2.5
S_{xx}^C	1180 ± 53
S_{yy}^C	173 ± 3.2
S_{zz}^C	165 ± 2.5
S_{xy}	106.9 ± 2.78
S_{xz}	97.87 ± 5.20
S_{yz}	35.21 ± 3.93

the failure load. Figure 6 shows Tsai-Hill failure contour plots for the $+45^\circ$, 0° , -45° and 90° plies at the mid-thickness (inner) and at the surface (outer) of the distributed QI tensile coupon. The plots in Figure 6 are for final failure of the 0° plies at a predicted load of ~ 637 kN. Failure within a ply is indicated by regions where the failure index has reached or exceeded a value of 1 (shown in red). It is noted that the 90° plies are the first plies to fail at low loads and therefore the Tsai-Hill contour plot in the region of the gauge-length is shown as 0. Final failure is predicted to occur in 0° plies near to the mid-thickness of the laminate and in the gauge-section shown in Figure 6. The outer plies show slightly higher (compared to the inner plies) Tsai-Hill index values near to the end-tab regions due to clamping effects. A similar analysis for the blocked QI tensile laminates predicts specimen final failure, in the 0° plies, to occur at ~ 558 kN.

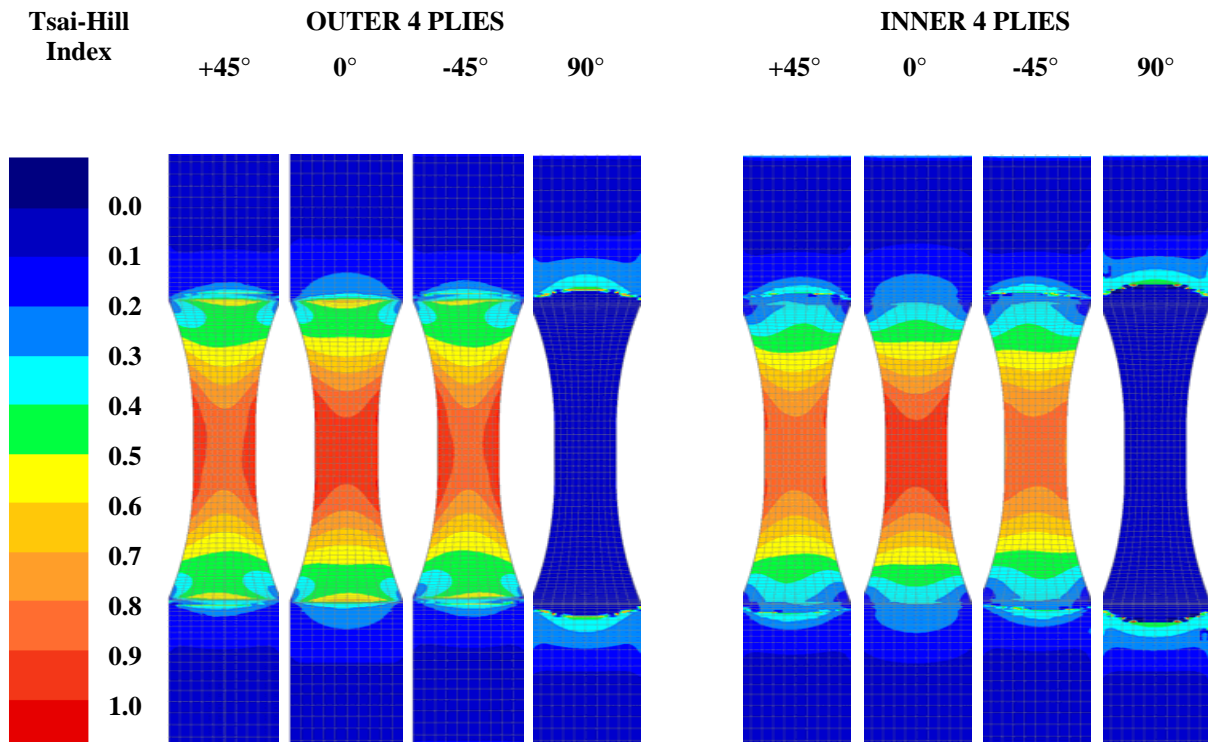


Figure 6: Tsai-Hill contour plots for outer and inner four plies for a distributed [+45°/0°/-45°/90°]_{ss} tensile specimen - load = 637 kN (N.B. an index of 1 represents failure)

PANEL & SPECIMEN PREPARATION

Fabrication of thick composite laminates (10 mm or greater) is often difficult, with process induced (i.e. residual) stresses becoming increasingly important as the thickness is increased. Residual stresses can have a significant effect on the engineering properties of laminated structures by inducing warpage, fibre buckling, matrix micro-cracking and delaminations. These stresses arise from resin chemical shrinkage, as a result of curing and differences in thermal contraction between adjacent plies on cooling the laminate from the cure temperature. The net effect is that the mechanical load required to induce failure is reduced.

Work was previously undertaken [4] to assess the effect of two different cure cycles on the physical, mechanical and thermal properties of sections of 20 mm thick CFRP material. Excessive exotherm (34.5°C above the cure temperature of 120°C) was observed for a 20 mm thick laminate cured according to the manufacturer’s recommended cure cycle (suitable for laminates <5 mm thick). An

optimised autoclave cure cycle was subsequently developed to minimise the temperature overshoot due to excessive exotherm and ensure an equivalent degree of cure between thin and thick laminates, thereby enabling direct comparison of thin and thick mechanical property data.

In order to obtain equivalent consolidation as for thin 8 and 16 ply laminates (as used in the manufacture of laminates for standard 2.5 and 5 mm thick tension and compression specimens, respectively), thick laminates were prepared by laying-up 4 plies at a time and then vacuum bag consolidating for 10 minutes, followed by adding a further 4 plies and again consolidating for 10 minutes. This process was repeated until a 64 ply laminate had been layed-up. Panels were then autoclave processed at NPL according to the optimised cure cycle detailed in [4] and shown schematically in Figure 7.

Specimens were extracted from cured panels using water jet profiling undertaken by GFM (UK) Ltd.

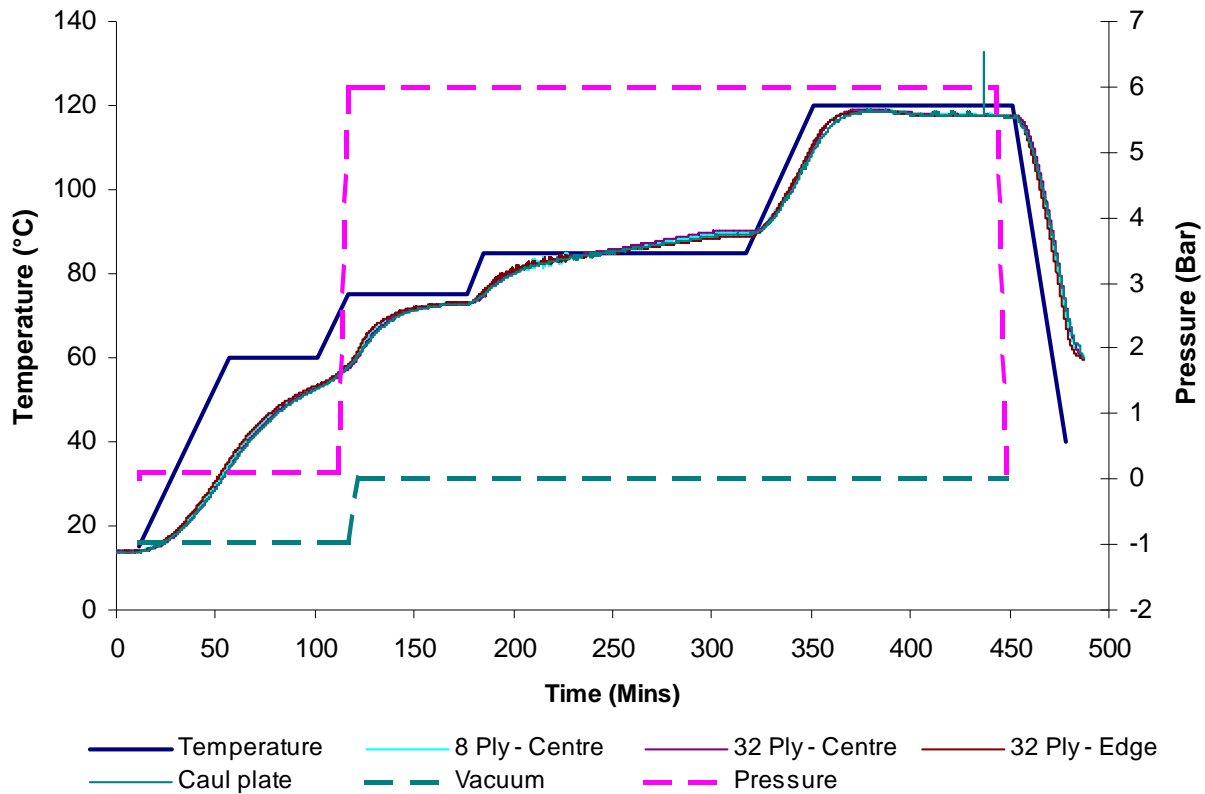


Figure 7: Autoclave and panel temperature distribution for a 64 ply laminate cured using the optimised cure cycle

On visual inspection of tensile coupons immediately after water jet machining, a series of cracks were observed in the surface $+45^\circ$ ply blocks. The cracks traversed the width of the coupons and were fairly regularly spaced (every 15-30 mm) along the coupon length (see Figure 8(a)). On closer inspection of the coupons it was noted that cracks were also present in the -45° , 90° and 0° ply blocks. In addition to visual inspection, X-ray radiography was also used to inspect an off-cut of the $[+45^\circ_8/0^\circ_8/-45^\circ_8/90^\circ_8]_s$ laminate from which the tensile coupons had been machined. The off-cut was soaked in a radio-opaque dye penetrant (zinc iodide solution) for 48 hours prior to X-ray inspection (25 kV and 3 mA tube voltage and current, respectively). Figure 8(b) clearly shows cracks present in all four ply orientations. The extensive degree of ply cracking observed in the $n = 8$ blocked QI laminate had a direct bearing on the choice of an $n = 4$ blocked laminate for the thick compression tests. Additional X-ray analyses were undertaken on the $n = 1$ (distributed) and $n = 4$ (blocked) laminates and no ply cracking was observed in either lay-up.

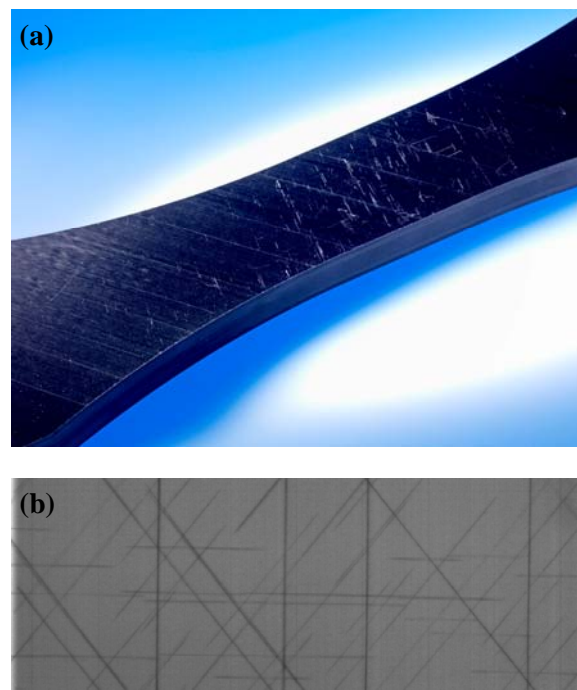


Figure 8: (a) image of cracking in the $+45^\circ$ ply blocks and (b) X-ray image of ply cracking in all ply orientations in the $[+45^\circ_8/0^\circ_8/-45^\circ_8/90^\circ_8]_s$ laminate

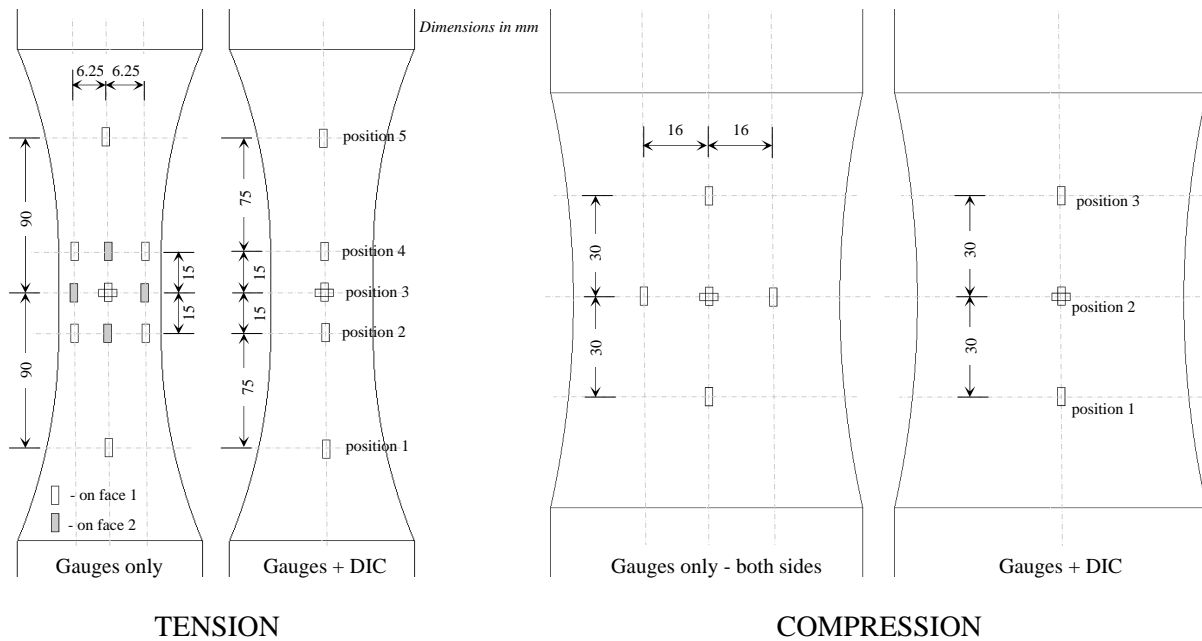


Figure 9: Strain gauge positions for tension and compression specimens

Individual tensile specimens were end-tabbbed after extraction from the mother panel using 5 mm thick Tufnol 10G/40@ woven glass fibre-reinforced epoxy material cut at 45° to the 0° fibre direction. End-tabs were bonded to the CFRP material using Scotchweld 9323 adhesive. Compression specimens were end-tabbbed prior to water jet machining to ensure that the ends of specimens were square.

MEASUREMENT OF STRAIN

Metal foil electrical-resistance gauges and digital image correlation (DIC) techniques were used to monitor strain (for modulus and degree of bending calculations and comparison with strain distributions predicted from FE analyses) for both tension and compression tests.

For the tension tests, one specimen per lay-up was extensively strain gauged on both sides of the coupon, whilst the remaining two specimens per lay-up were gauged on only one side, the other side left blank so that it could be analysed using DIC. Similarly, for the compression tests, three specimens per lay-up were strain gauged on both sides whilst the remaining three specimens were gauged on one side with the other used for DIC analysis. A combination of 5 mm gauge length uni-axial and biaxial strain gauges were used for both

tension and compression specimens. Gauge positions for tension and compression specimens are shown in Figure 9 and a fully gauged tensile specimen is shown in Figure 10.

DIC is a non-contact full-field strain measurement technique. The basic concept of DIC is to compare images of a component before and after deformation. Displacements

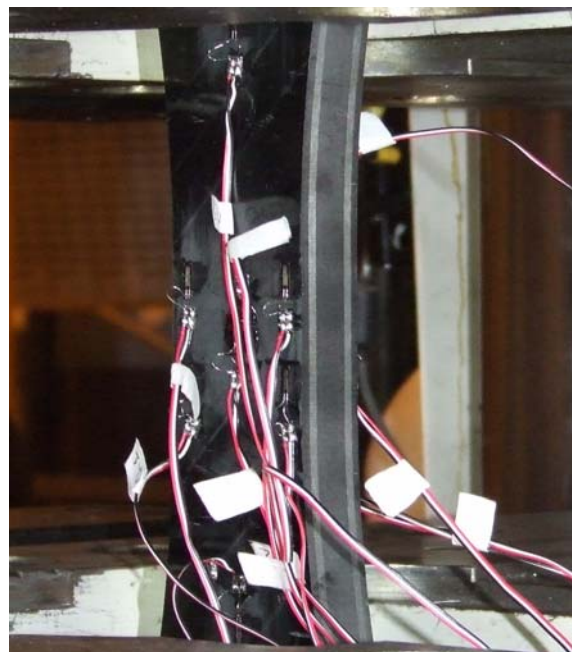


Figure 10: A strain gauged tensile coupon

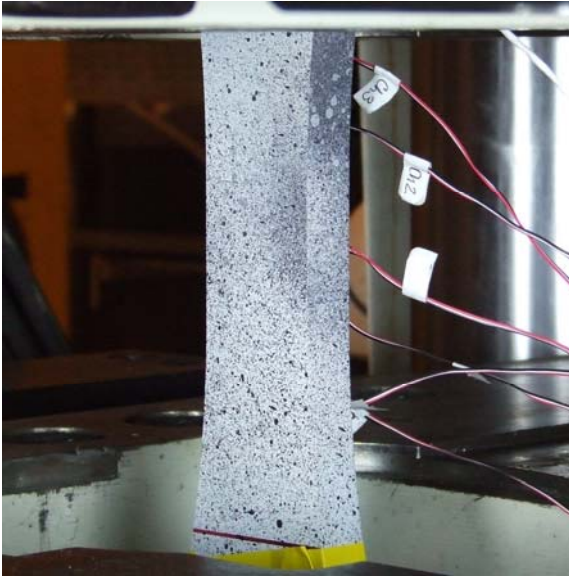


Figure 11: Speckle pattern sprayed onto the specimen surface for DIC analysis

and strains are determined by correlating the position of pixel subsets or blocks in the original and deformed images, normally based upon contrast i.e. grey intensity levels. The size of the pixel block can be varied, thus allowing many random patterns to be correlated. In order to identify if there is any movement between the two blocks there must be sufficient detail for it to be considered unique. It may be the case that the specimen or component already has a suitable level of surface features which can be imaged directly, but if not, some form of spray paint or coating or scratches on the surface can be used. Specimens that were analysed with DIC were sprayed with white, grey and black paint to achieve a unique surface finish with a variety of grey levels (Figure 11). A LaVision[®] system with two 5 megapixel video cameras was used to map 2D strain distributions. For all of the specimens that were selected for DIC strain measurements, one face and one edge of the coupons were sprayed ready for DIC inspection. Images were recorded at a frequency of 1 Hz throughout the tests and all strain results were calculated relative to the first image recorded at zero load.

DETAILS OF MECHANICAL TESTING

Tension

Tensile tests were undertaken using a 2 MN Dartec hydraulic test machine at Qinetiq,

Farnborough. Specimens were clamped using hydraulic grips to ensure even gripping pressure (200 bar) across the end-tabbed regions. All tests were undertaken at a crosshead displacement rate of 2 mm/minute which is the same rate as for the 2.5 mm thick QI specimens. Load, crosshead displacement, strain and DIC images were recorded continuously throughout each test until final failure of the specimen had occurred. Strain readings were used to monitor axial and through-thickness bending throughout the tests as per the bending criteria recommended in [1]. The acceptable level of bending according to this criteria is 3% or less.

Compression

For data generated for ~20 mm thick specimens to be comparable to the ~5 mm thick QI data, the method of compression loading for the thick specimens was end-loading as opposed to shear loading as used in the IITRI and Celanese jigs [5]. It is noted that end-loading jigs predominantly apply compressive load through end-loading but there is a degree of shear loading present due to initial clamping of the end-tab regions and through-thickness Poisson's expansion as the compressive load is increased.

Tests were conducted using a large, four pillar die set end-loading compression jig designed and manufactured at National Physical Laboratory (NPL). This jig (Figure 12) is capable of loading specimens up to 90 mm wide and ~300 mm long in compression. For the $n = 4$ blocked QI specimens, the failure load was anticipated to be ~400-450 kN. Tests were conducted using an Instron 1197 screw-driven machine fitted with a 500 kN load cell. For the $n = 1$ distributed QI specimens, the failure load was anticipated to be ~520-560 kN and therefore tests were undertaken on a 600 kN Avery hydraulic compression test machine. The same compression jig was used on both machines and the alignment of the jig on the test machine was set using a ground steel bar, in place of the specimen, to ensure that the top and bottom loading blocks were correctly aligned. Each loading block contains a recess in which sits a clamping plate (Figure 13). The clamping plate is used to hold the specimen centrally in the loading block and provides lateral constraint to the end-tabbed



Figure 12: Large four pillar die set used for end-loaded compression tests

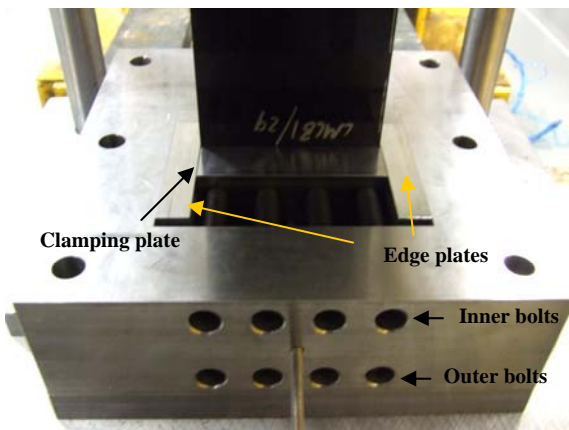


Figure 13: Close up of lower loading block with clamping plate and locking bolts

regions of the specimen. Two rows of four bolts are used to apply clamping pressure to the specimen via the clamping plate. With the specimen in place, the inner row of bolts was torqued to 5 Nm and the outer rows of bolts was torqued to 10 Nm. It is noted that the specimen sits between two edge plates with an interference fit. The edge plates provide edge constraint to the end-tabbed regions of the specimen.

Compression tests were undertaken at a crosshead displacement rate of 1 mm/minute, which was the same rate at which the 5 mm

thick QI specimens were tested. Load, crosshead displacement, strain gauge and DIC images were recorded continuously throughout each test until final failure of the specimen had occurred. Readings from opposing pairs of strain gauges were used to monitor the degree of bending. The criteria used was the same as that recommended in ISO 14126 [2] i.e. the difference between opposing pairs of gauges must be less than 10% throughout the compression test.

RESULTS

Tension

The sub-laminate scaled, distributed QI specimens failed at a mean load of 533 kN and had a fairly linear load-deflection response up to failure (Figure 14). Failure in all specimens was sudden with little damage occurring before final failure. The level of total bending (axial and through-thickness) in all three specimens was less than 3%.

A mean failure load of 386 kN was achieved for the three ply-level scaled, blocked QI specimens. Extensive ply cracking and delamination formation was observed throughout the tests, with fibre failure occurring near to failure. Due to the amount of initial ply cracking in the outer +45° ply blocks, the use of strain gauges did not prove to be successful for monitoring bending or determination of axial modulus. The load-deflection response for blocked QI specimens was non-linear and indicative of the progressive nature of damage formation throughout the test.

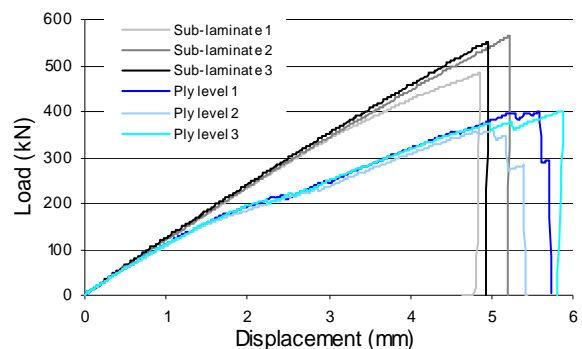


Figure 14: Load vs. displacement for thick tension tests



Figure 15: Failed thick tensile coupons: (a) distributed QI and (b) blocked QI

All distributed and blocked specimens failed within the gauge section away from the end-tabs - see Figure 15. The individual tensile property results are detailed in Table 4. The modulus and Poisson’s ratio values for the

Table 5: Comparison of ϵ_{xx} and ϵ_{yy} Strains (%) for the Front Face of a Thick, Distributed QI Tension Specimen

Position	Strain Gauge		DIC		FEA	
	ϵ_{xx}	ϵ_{yy}	ϵ_{xx}	ϵ_{yy}	ϵ_{xx}	ϵ_{yy}
1	0.95	-	1.03	-	0.95	-
2	1.12	-	1.14	-	1.21	-
3	1.11	-0.38	1.13	-0.40	1.23	-0.34
4	1.14	-	1.15	-	1.21	-
5	0.94	-	1.04	-	0.95	-

blocked specimens are indicative only, due to the level of initial cracking seen in the outer +45° ply blocks. The tensile strengths for the distributed and blocked specimens were measured as 540 and 392 MPa, respectively. This represents a 27% reduction in strength due to n = 8 ply blocking.

A comparison of measured strains (at 5 positions as detailed in Figure 9) using strain gauges and DIC to predicted values from FEA is shown in Table 5. DIC strain values are mean values sampled over an area equivalent to that of a 5 mm strain gauge. The level of agreement between gauges, DIC and FEA was very good for all positions.

Table 4: Individual Tensile Results

Scaling Type	Specimen	Modulus (GPa)	Poisson’s ratio	Max. Load (kN)	Strength (MPa)
Sub-laminate (n = 1)	ABSN001	45.6	0.33	484	490
	ABSN002	45.1	0.34	564	571
	ABSN003	46.0	0.33	551	560
	<i>Mean (SD, CoV)</i>	<i>45.6 (0.5, 1%)</i>	<i>0.33 (0.01, 1.7%)</i>	<i>533 (43, 8%)</i>	<i>540 (44, 8%)</i>
Ply-level (n = 8)	ABSM001	36.9	0.58	399	406
	ABSM002	28.2	0.41	358	364
	ABSM003	38.8	0.57	401	407
	<i>Mean (SD, CoV)</i>	<i>34.6 (5.7, 16%)</i>	<i>0.52 (0.1, 18%)</i>	<i>386 (24, 6%)</i>	<i>392 (25, 6%)</i>

N.B. Figures in grey font are indicative only due to ply cracking observed in specimens prior to loading

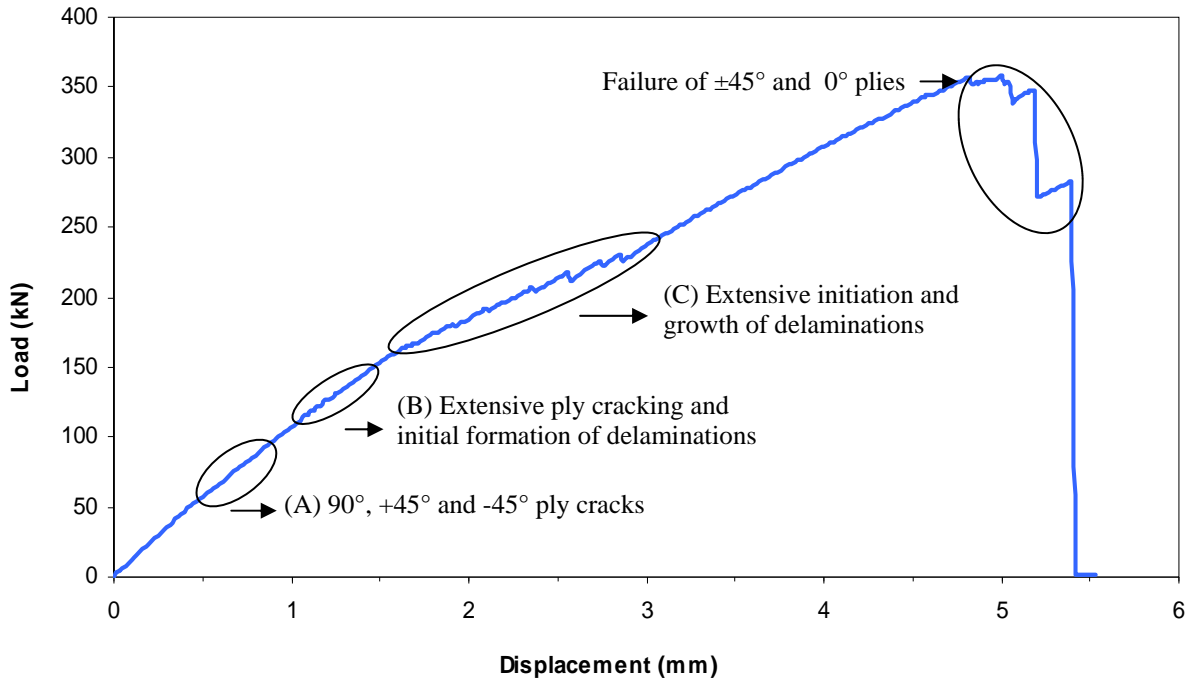


Figure 16: Failure progression in thick, blocked tensile laminate

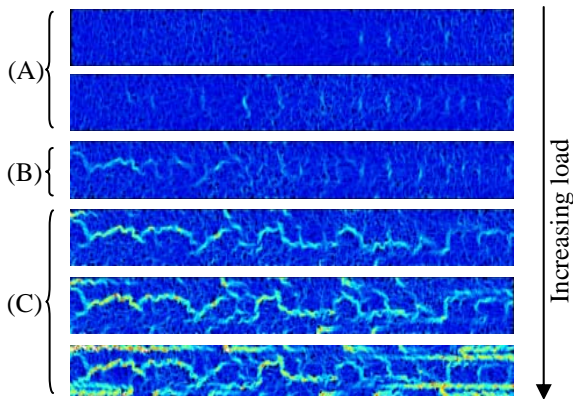


Figure 17: Images of max. normal strain by DIC of thick tensile specimen edges

Figure 16 shows the load-deflection response for an individual blocked coupon together with a summary of the predominant damage mechanisms at various stages throughout the test. DIC was used to monitor the strain distribution on the edge of blocked tensile coupons and to provide more information on the formation of damage. Figure 17 shows a series of plots of maximum normal strain distributions (from DIC) on the edge of a thick blocked specimen. The two plots corresponding to region ‘A’ on the curve in Figure 16 show the opening of pre-existing 90° ply cracks and the formation of new cracks in the +45°, -45° and 90° ply blocks. Without DIC analysis, these ply cracks would

not have been visible to the naked eye. The strain plot for region ‘B’ shows the formation of extensive ply cracking and also the onset of delamination. The region ‘C’ plots show the extensive degree of delamination initiation and propagation as the test progresses. It is noted that DIC analysis of the edge of the distributed coupons did not show damage formation until just prior to failure when sudden delamination was seen between the outer plies.

Compression

Typical load-deflection plots for compression tests on distributed and blocked QI lay-ups are shown in Figure 18. Initially the response is non-linear as ‘slack’ is taken up in the loading

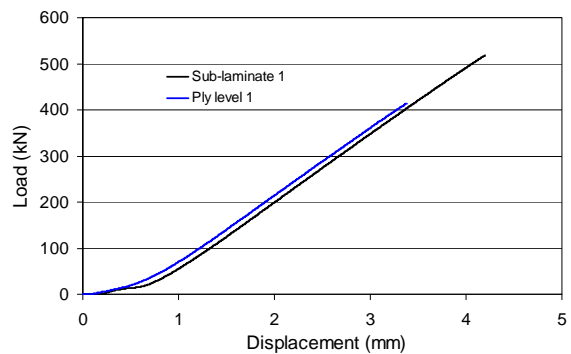


Figure 18: Load vs. displacement for thick compression tests

train. The plots for both lay-up types are then linear up to failure. The sub-laminate scaled, distributed QI specimens failed at a mean load of 559 kN and failure in all specimens was sudden with little damage occurring before final failure. A mean failure load of 421 kN was achieved for the ply-level scaled, blocked QI specimens, and as with the distributed lay-up specimens, failure in all specimens was sudden with little damage occurring before final failure.

All distributed and blocked specimens failed within the gauge-section away from the end-tabs - see Figure 19. The degree of bending in all fully strain gauged specimens was less than 10%. Individual compressive property results are detailed in Table 6. The compressive strengths for the distributed and blocked specimens were measured as 456 and 336 MPa, respectively. This represents a 26% reduction in strength due to $n = 4$ ply blocking. Modulus and Poisson's ratio values for the distributed and blocked lay-ups were in good agreement.

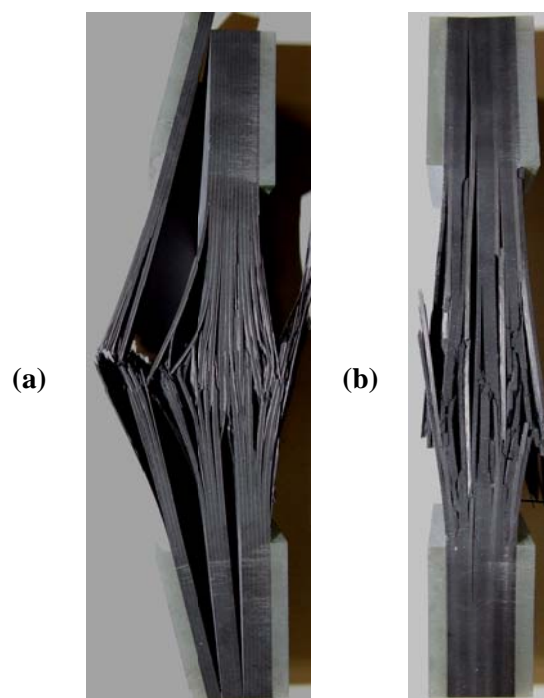


Figure 19: Failed compression specimens; (a) distributed QI and (b) blocked QI

Table 6: Individual Compressive Results

Scaling Type	Specimen	Max. Bending (%) ¹	Modulus (GPa)	Poisson's ratio	Max. Load (kN)	Strength (MPa)
Sub-laminate (n = 1)	ABXM001	2.8	43.5	0.27	523*	414*
	ABXM002	9.5	41.7	0.28	554	439
	ABXM003	-	43.3	0.28	515	407
	ABXM004	-	42.5	0.27	559	446
	ABXM005	2.0	41.9	0.28	553	442
	ABXM006	-	36.7*	0.37*	571	456
	<i>Mean (SD, CoV)</i>	-	<i>42.6 (0.8, 1.9%)</i>	<i>0.28 (0.01, 2.0%)</i>	<i>559 (8, 2%)</i>	<i>446 (7, 2%)</i>
Ply-level (n = 4)	ABYA001	-	41.2	0.31	414	332
	ABYA002	0.2	41.6	0.31	388	312
	ABYA003	-	41.9	0.28	452	362
	ABYA004	3.1	42.3	0.29	414	328
	ABYA005	4.6	41.9	0.30	421	335
	ABYA006	-	38.9*	0.29	436	346
	<i>Mean (SD, CoV)</i>	-	<i>41.8 (0.4, 1.0%)</i>	<i>0.30 (0.01, 3.5%)</i>	<i>421 (22, 5%)</i>	<i>336 (17, 5%)</i>

¹ - maximum bending calculated from mean values of strain on opposing gauge pairs,

* - data removed as outliers after statistical analysis

N.B. Figures in grey font were not included in statistical analysis due to partial delamination seen in specimen prior to loading.

Table 7: Comparison of ϵ_{xx} and ϵ_{yy} Strains (%) for a Thick, Distributed QI Compression Specimen

Position	Strain Gauge		DIC		FEA	
	ϵ_{xx}	ϵ_{yy}	ϵ_{xx}	ϵ_{yy}	ϵ_{xx}	ϵ_{yy}
1	-1.05	-	-0.89	-	-0.91	-
2	-1.02	0.29	-0.97	0.29	-0.93	0.26
3	-0.99	-	-1.00	-	-0.91	-

Comparisons of measured strains (at 3 positions as detailed in Figure 9) using strain gauges and DIC to predicted values from FEA are shown in Tables 7 and 8 for distributed and blocked specimens, respectively. DIC strain values are mean values sampled over an area equivalent to that of a 5 mm strain gauge. As for the tensile coupons, the level of agreement between gauges, DIC and FEA was good for all positions.

DISCUSSION AND CONCLUSIONS

Thick section specimen designs for both tension and compression testing were successfully evaluated and resulted in valid failure modes. The use of DIC for full-field strain measurements was successful and proved to be a useful tool for detecting and monitoring damage formation in thick, blocked tensile coupons.

Table 8: Comparison of ϵ_{xx} and ϵ_{yy} Strains (%) for a Thick, Blocked QI Compression Specimen

Position	Strain Gauge		DIC		FEA	
	ϵ_{xx}	ϵ_{yy}	ϵ_{xx}	ϵ_{yy}	ϵ_{xx}	ϵ_{yy}
1	-0.97	-	-0.99	-	-0.83	-
2	-0.92	0.28	-0.93	0.27	-0.84	0.25
3	-0.87	-	-0.99	-	-0.83	-

A summary of the thick-section tensile and compression results are detailed in Tables 9 and 10, respectively. The tables provide a comparison with data generated from ‘thin’ coupons as per ISO 527-4 [1] and ISO 14126 [2] for tensile and compressive data, respectively. For the distributed QI lay-up, the tensile and compression modulus, Poisson’s ratio (where possible) and strength results are in good agreement with the standard ‘thin’ data. This would suggest that there is no geometric scaling effect between the standard thickness (2.5 and 5 mm) and ~20 mm thick laminates.

For the blocked QI lay-up, the tensile and compression modulus and Poisson’s ratio values (where possible) were in good agreement with the standard ‘thin’ data. However, the strength values were 27% and 26% lower than the ‘thin’ data for n = 8

Table 9: Summary of Tension Results

Lay-up details		Nominal Thickness (mm)	Modulus (GPa)	Poisson’s ratio	Strength (MPa)
Standard (thin)	[+45°/0°/-45°/90°] _s	2.5	44.2 ± 0.6	0.35 ± 0.03	551 ± 22
Distributed (thick)	[+45°/0°/-45°/90°] _{8s}	20	45.6 ± 0.5	0.33 ± 0.01	540 ± 44
Blocked (thick)	[+45° ₈ /0° ₈ /-45° ₈ /90° ₈] _s	20	34.6 ± 5.7	0.52 ± 0.10	392 ± 25

Table 10: Summary of Compression Results

Lay-up details		Nominal Thickness (mm)	Modulus (GPa)	Poisson’s ratio	Strength (MPa)
Standard (thin)	[+45°/0°/-45°/90°] _{2s}	5	44.0 ± 2.4	-	454 ± 12
Distributed (thick)	[+45°/0°/-45°/90°] _{8s}	20	42.6 ± 0.8	0.28 ± 0.01	446 ± 7
Blocked (thick)	[+45° ₄ /0° ₄ /-45° ₄ /90° ₄] _{2s}	20	41.8 ± 0.4	0.30 ± 0.01	336 ± 17

(tension) and $n = 4$ (compression) ply blocked laminates, respectively.

The reduction in strength (tension and compressive) of blocked, compared to distributed, laminates has been extensively reported [6-9]. It is widely accepted that matrix cracking initiates at lower strains as the ply block thickness increases. This was clearly evident in the $n = 8$ laminates, where ply cracks formed at zero axial strain. It has also been shown [10] that interlaminar stresses arise at the edges of laminates with differing ply orientations. The magnitude of these interlaminar stresses can cause edge delamination at lower strains. Delamination of the $n = 8$ blocked tensile laminates was seen to initiate on the edges of coupons at low levels of strain. The effects of the stresses decay rapidly with increasing distance from the free edge - typically the thickness of a ply block. Thus, for an $n = 8$ blocked laminate, interlaminar stresses effect a larger area than for the $n = 1$ laminate and trigger the onset of edge delamination at lower loads.

Additional work is currently being undertaken at NPL to predict the formation, prior to loading, of ply cracks in heavily ply blocked multi-directional laminates. This phenomena is thought to be due to a combination of residual stress formation during cure, the onset of matrix cracking and the creation of interlaminar stresses at newly created free edges after machining. Initial results (to be published) using the LUSAS High Precision Moulding software to predict the levels of residual stress in distributed and blocked laminates, have shown that the levels of residual stress in both lay-ups are approximately the same. It is thought that the ply cracking in blocked laminates is due to the residual stress acting over a larger area i.e. thick ply block, compared to the distributed lay-up and also the level of constraint afforded by adjacent plies (weaker for thicker ply blocks).

From a testing perspective, the requirement to characterise thick-section mechanical properties is not an in-expensive activity. The shear size and thickness of specimens requires significant amounts (at least an order of magnitude greater than for standard thin test

pieces) of material and man-hours to prepare. Large capacity loading machines and gripping mechanisms (for tension testing) are specialist pieces of equipment, extremely expensive and not common place in many engineering organisations. In addition, specialist loading jigs e.g. the end-loading compression jig, are required which also add to the considerable cost of testing. The results of this study have indicated that for thick sections of the same base unit lay-up as that used in standard thickness coupons, it may not be necessary to undertake thick section testing as the thick and thin data have been shown to be equivalent (for tension and compression). However, if ply blocking in thick sections is used then it is highly recommended that thick section tests are undertaken as significant strength reductions have been shown to result. It is emphasised that, for these very reasons, the level of ply blocking used in this study is not typical of that used in many engineering applications, but was chosen to highlight the effects of ply blocking in laminated composites.

REFERENCES

1. ISO 527-4 Plastics – Determination of Tensile Properties. Part 4: Test Conditions for Isotropic and Orthotropic Fibre-Reinforced Plastic Composites”.
2. ISO 14126 Fibre-Reinforced Plastic Composites - Determination of Compressive Properties in the In-plane Direction.
3. ASTM D 3039 - Standard Test Method for Tensile Properties of Polymer Matrix Composite Materials
4. M. R. L. Gower, R.M. Shaw. and W. R. Broughton, “Thick Composites: Part I: Mechanical Test Review, Part II: Cure Optimisation”, NPL Report MAT 24, April 2008.
5. R. M. Shaw and G. D. Sims, “Understanding Compression Testing of Thick Polymer Matrix Composites”, NPL Measurement Note DEPC-MN 019, April 2005.
6. Lagace, P., Brewer, J. and Kassapoglou, C., (1987) “The Effect of Thickness on Interlaminar Stress and Delamination in Straight Edged Laminates”, Journal of Composites Technology and Research, 9: 81-87.
7. Kellas, S. and Morton, J. “Strength Scaling in Fiber Composites”, NASA CR 4335, November 1990.
8. Jackson, K.E., Kellas, S. and Morton, J. “Scale Effects in the Response and Failure of Fiber Reinforced Composite Laminates Loaded in Tension and in Flexure”, Journal of Composite Materials, Vol.26, No. 18, 1992, pp.2674-2705.
9. Kellas, S. and Morton, J. “Scaling Effects in Angle-Ply Laminates”, NASA CR 4423, February 1992.
10. Pipes, R.B. and Pagano, N.J. (1970). Interlaminar Stresses in Composite Laminates Under Uniform Axial Extension, Journal of Composite Materials, 4: 538-548.

ACKNOWLEDGEMENTS

The research reported in this Measurement Note was carried out at NPL as part of the Characterisation Programme funded by the United Kingdom Department of Innovation, Universities and Skills (National Measurement System Directorate). The authors would like to express their gratitude to the Industrial Advisory Group, Gurit Holdings AG, Qinetiq, and NPL colleagues Dr Bill Broughton and Dr Graham Sims.

For further information contact:

Mr Michael Gower
Biomaterials, Polymers and Composites Group
Industry and Innovation Division
National Physical Laboratory
Hampton Road, Teddington
Middlesex
TW11 0LW
Telephone: 020-8977 3222 (*switchboard*)
Direct Line: 020-8943 8625
Facsimile: 020-8943 6177